hep-ph/0304245

On the Complementarity of Higgs and Radion Searches at LHC

Marco Battaglia[1], **Stefania De Curtis**[2], **Albert De Roeck**[1],
Daniele Dominici[2,3] and **John F. Gunion**[4]

[1] *CERN, Geneva (Switzerland)*

[2] *INFN, Sezione di Firenze (Italy)*

[3] *Universita' degli Studi di Firenze, Dip. di Fisica (Italy)*

[4] *University of California, Davis CA (USA)*

Abstract

Models with 3-branes in extra dimensions typically imply the existence of a radion, ϕ, that can mix with the Higgs, h, thereby modifying the Higgs properties and the prospects for its detectability at the LHC. The presence of the ϕ will extend the scope of the LHC searches. Detection of both the ϕ and the h might be possible. In this paper, we study the complementarity of the observation of $gg \to h$, with $h \to \gamma\gamma$ or $h \to Z^0 Z^{0*} \to 4\ \ell$, and $gg \to \phi \to Z^0 Z^{0(*)} \to 4\ \ell$ at the LHC in the context of the Randall-Sundrum model. The potential for determining the nature of the detected scalar(s) at the LHC and at an e^+e^- linear collider is discussed, both separately and in combination.

25 April 2003

1 Introduction

By the end of this decade we expect that the quest for the Higgs boson, responsible for electro-weak symmetry breaking and mass generation, will be successfully completed, thanks to the data provided by the LHC hadron collider. A significant effort has been put into the design and optimization of the ATLAS and CMS detectors to match the characteristics of the expected Higgs signals. However fundamental, discovery of one or more Higgs-like particles might leave unanswered the question of the hierarchy between the electroweak scale, defined by the Higgs vacuum expectation value v =246 GeV, and the Planck scale. In an attempt to solve this problem, without necessarily relying on supersymmetry, theories with extra dimensions have been proposed. These theories have become the focus of a fascinating program of planned investigations.

One particularly attractive extra-dimensional model is that proposed by Randall and Sundrum (RS) [1], in which there are two 3+1 dimensional branes separated in a 5th dimension. A central prediction of this theory is the existence of the radion, a graviscalar which corresponds to fluctuations in the size of the extra dimension. Detection and study of the radion will be central to the experimental probe of the RS and related scenarios with extra dimensions. There is already an extensive literature on the phenomenology of the radion, both in the absence of Higgs-radion mixing [2–6] and in the presence of such a mixing [7–13].

In this paper we discuss the complementarity of the search for the Higgs boson and the radion at the LHC. As the Higgs-radion mixing may suppress the main discovery process $gg \to H \to \gamma\gamma$ for a light Higgs boson, we study the extent to which the appearance of a $gg \to \phi \to Z^0 Z^{0(*)} \to 4\ \ell$ signal ensures that LHC experiments will observe at least one of the two scalars over the full parameter phase space. The additional information, which could be extracted from a TeV-class e^+e^- linear collider (LC), is also considered.

2 Curvature-Scalar mixing and Radion Phenomenology

In the simplest version of the 5-dimensional RS model, all the SM particles and forces, with the exception of gravity, are confined to one of the 4-dimensional boundaries. Gravity lives on this visible brane, on the second hidden brane and in the 5-dimensional compactified bulk. All mass scales in the 5-dimensional theory are of the order of the Planck mass. By placing the SM fields on the visible brane, all the terms of order of the Planck mass are rescaled by an exponential suppression factor $\Omega_0 \equiv e^{-m_0 b_0/2}$, which is called the warp factor. This reduces the mass scales on the visible brane down to the weak scale $\mathcal{O}$(1 TeV) without any severe fine tuning. A ratio of 1 TeV/M_{Pl} (where M_{Pl} is the reduced Planck mass, $M_{Pl} \sim 2.4 \times 10^{18}$ GeV) corresponds to $m_0 b_0/2 \sim 35$.

In the RS model, a mixing between the radion field and the Higgs field $\widehat{H}$ is induced by the following action [14]:

$$S_\xi = \xi \int d^4x \sqrt{g_{\rm vis}} R(g_{\rm vis}) \widehat{H}^\dagger \widehat{H}\,, \tag{1}$$

where $R(g_{\rm vis})$ is the Ricci scalar for the metric induced on the visible brane, $g^{\mu\nu}_{\rm vis} = \Omega_0^2\Omega^2(x)(\eta^{\mu\nu}+\epsilon h^{\mu\nu})$ and ξ a dimensionless parameter. After rescaling $H_0 = \Omega_0\widehat{H}$, and making the usual shifts [$H_0 = \frac{1}{\sqrt{2}}(v+h_0)\,,\ \ \Omega(x) = 1+\frac{\phi_0}{\Lambda_\phi}$, with $v = 246$ GeV] the following kinetic energy terms are found:

$$\mathcal{L} = -\tfrac{1}{2}\left\{1+6\gamma^2\xi\right\}\phi_0\Box\phi_0 - \tfrac{1}{2}\phi_0 m^2_{\phi_0}\phi_0 - \tfrac{1}{2}h_0(\Box + m^2_{h_0})h_0 - 6\gamma\xi\phi_0\Box h_0\,, \tag{2}$$

where m_{h_0} and m_{ϕ_0} are the Higgs and radion masses before mixing, and $\gamma \equiv v/\Lambda_\phi$.

The states that diagonalize the kinetic energy and have canonical normalization are h and ϕ with:

$$h_0 = \left(\cos\theta - \frac{6\xi\gamma}{Z}\sin\theta\right)h + \left(\sin\theta + \frac{6\xi\gamma}{Z}\cos\theta\right)\phi \equiv dh + c\phi \tag{3}$$

$$\phi_0 = -\cos\theta\frac{\phi}{Z} + \sin\theta\frac{h}{Z} \equiv a\phi + bh\,. \tag{4}$$

Here, the mixing angle θ is given by

$$\tan 2\theta \equiv 12\gamma\xi Z\frac{m^2_{h_0}}{m^2_{\phi_0} - m^2_{h_0}(Z^2 - 36\xi^2\gamma^2)}\,, \tag{5}$$

and

$$Z^2 \equiv 1 + 6\xi\gamma^2(1-6\xi)\,. \tag{6}$$

The couplings of the h and ϕ to ZZ, WW and $f\overline{f}$ are given relative to those of the SM Higgs boson, denoted by H, by:

$$\frac{g_{hW^+W^-}}{g_{HW^+W^-}} = \frac{g_{hZ^0Z^0}}{g_{HZ^0Z^0}} = \frac{g_{hf\overline{f}}}{g_{Hf\overline{f}}} = d + \gamma b\,, \quad \frac{g_{\phi W^+W^-}}{g_{HW^+W^-}} = \frac{g_{\phi Z^0Z^0}}{g_{HZ^0Z^0}} = \frac{g_{\phi f\overline{f}}}{g_{Hf\overline{f}}} = c + \gamma a\,. \tag{7}$$

Couplings of the h and ϕ to $\gamma\gamma$ and gg receive contributions not only from the usual loop diagrams but also from trace-anomaly couplings of the ϕ_0 to $\gamma\gamma$ and gg. Thus, these couplings are not simply directly proportional to those of the SM H. Of course, in the limit of $\xi = 0$, the h has the same properties as the SM Higgs boson.

In the end, when $\xi \neq 0$ the four primary independent parameters are: ξ, Λ_ϕ and the mass eigenvalues m_h and m_ϕ. These completely determine a, b, c, d and, hence, all the couplings of the h and ϕ to W^+W^-, Z^0Z^0 and $f\overline{f}$ — see Eq. (7). One further parameter is required to completely fix the h and ϕ decay phenomenology in the RS model: m_1, the mass of the first KK graviton excitation, given by

$$m_1 = x_1\frac{m_0}{M_{Pl}}\frac{\Lambda_\phi}{\sqrt{6}} \tag{8}$$

where m_0 is the curvature parameter and x_1 is the first zero of the Bessel function J_1 ($x_1 \sim 3.8$).

Current bounds, derived from Tevatron Run I data and precision electroweak constraints have been examined in Ref. [5]. Lower bounds on the radion mass, from Higgs searches at LEP, are weak. In particular, the ϕZ^0Z^0 coupling given in Eq. (7) remains small relative to the SM HZ^0Z^0 coupling for low radion masses [13].

3 Higgs and Radion Searches at LHC

The search for the Higgs boson represents one of the most crucial goals for the LHC physics program. If the SM H is light, as present precision electroweak data suggest, the single most promising LHC discovery channel is $gg \to H \to \gamma\gamma$. Rather detailed studies of the significance of a Higgs signal using inclusive production have been carried out for the ATLAS [15] and CMS [16] experiments. Results are summarized in Figure 1. The $H \to \gamma\gamma$ channel appears to be instrumental for obtaining a $\geq 5\sigma$ signal at low luminosity, if 115 GeV $< M_H <$ 130 GeV. The $t\bar{t}H$, $H \to b\bar{b}$ and $H \to Z^0 Z^{0*} \to 4\ \ell$ channels also contribute, with lower statistics but a more favourable signal-to-background ratio. Preliminary results, also shown in Figure 1, indicate that Higgs boson production in association with forward jets may also be considered as a discovery mode. However, here the background suppression strongly relies on the detailed detector response.

Studies for dedicated searches of radions at the LHC have also been carried out. In particular, the study in ref. [11] has obtained discovery limits using both the $\phi \to \gamma\gamma$ and the $\phi \to Z^0 Z^{0(*)} \to 4\ell$ processes by re-interpreting the corresponding H decay channels. The more intriguing process $\phi \to HH$ has also been considered, limited to the $\gamma\gamma b\bar{b}$ final state.

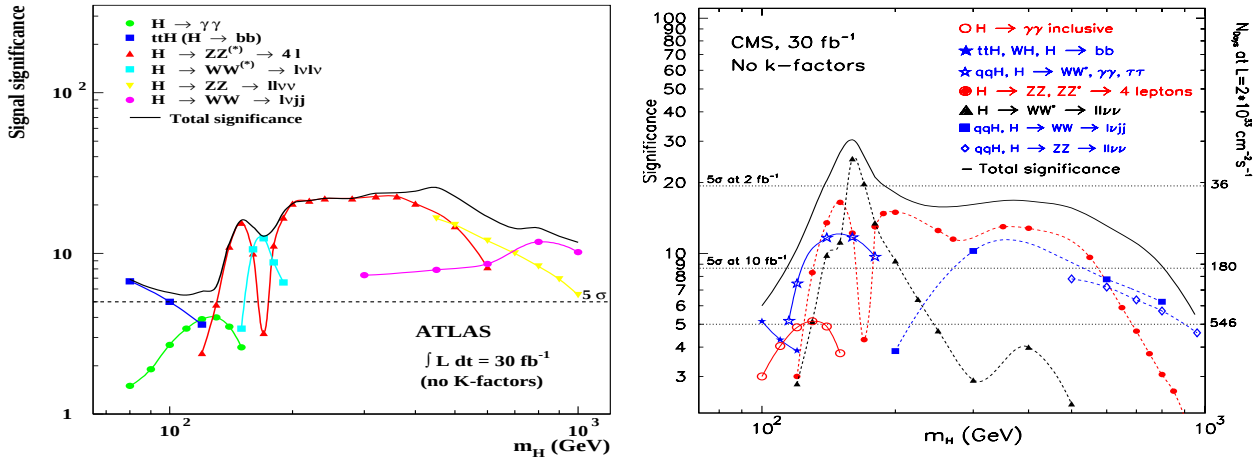

Figure 1: *Higgs signal significance as function of the Higgs boson mass. The curves show the signal significance for an integrated luminosity of 30 fb^{-1} for* ATLAS *[15] (left) and* CMS *[16] (right). In the right plot the contributions from the qqH channel are also shown. No K-factors have been included.*

A more subtle aspect of theories with warped extra dimensions is the effect of the Higgs-radion mixing [10, 12, 13], which can modify the production and decay properties of the Higgs boson to weaken, or even invalidate, the expectations for Higgs observability obtained so far.

4 Complementarity and Distinguishability

In this section, we address two issues. The first is whether there is a complementarity between the Higgs observability, mostly through $gg \to h \to \gamma\gamma$, and the $gg \to \phi \to Z^0 Z^{0(*)} \to 4\ \ell$ reaction, thus

offering the LHC the discovery of at least one of the two particles over the full parameter space. The second, and related, issue concerns the strategies available to understand the nature of the discovered particle.

The effects of the mixing of the radion with the Higgs boson have been studied [13] by introducing the relevant terms in the HDECAY program [17], which computes the Higgs couplings, including higher order QCD corrections. Couplings and widths for the radion have also been implemented. We consider the range 50 GeV $< M_\phi <$ 300 GeV, whose lower end is consistent with present bounds derived from LEP data. We will also focus on cases for which M_h is not very large, as possibly most consistent with precision electroweak constraints.

Results have been obtained by comparing the product of production and decay rates to those expected for a light SM H. The LHC sensitivity has been extracted by rescaling the results for Higgs observability, obtained assuming SM couplings. We define the Higgs observability as $> 5\ \sigma$ excess over the SM background for the combination of the inclusive channels: $gg \to h \to \gamma\gamma$; $t\bar{t}h$, $h \to b\bar{b}$ and $h \to Z^0 Z^{0(*)} \to 4\ell$, as given in the left panel of Figure 1. We study the results as a function of four parameters: the Higgs mass M_h, the radion mass M_ϕ, the scale Λ_ϕ and the mixing parameter ξ.

4.1 Radion and Higgs Boson Search Complementarity

Due to the suppression, from radion mixing, of the loop-induced effective couplings of the h (relative to the SM H) to gluon and photon pairs, the key process $gg \to h \to \gamma\gamma$ may fail to provide a significant excess over the $\gamma\gamma$ background at the LHC. Other modes that depend on the gg fusion production process are suppressed too. For $M_\phi > M_h$, this suppression is very substantial for large, negative values of ξ. This region of significant suppression becomes wider at large values of M_ϕ and Λ_ϕ. In contrast, for $M_\phi < M_h$, the $gg \to h \to \gamma\gamma$ rate is generally only suppressed when $\xi > 0$. All this is shown, in a quantitative way, by the contours in Figures 2 and 3. The outermost, hourglass shaped contours define the theoretically allowed region. Three main regions of non-detectability may appear. Two are located at large values of M_ϕ and $|\xi|$. A third region appears at low M_ϕ and positive ξ, where the above-noted $gg \to h \to \gamma\gamma$ suppression sets in. It becomes further expanded when $2M_\phi < M_h$ and the decay channel $h \to \phi\phi$ opens up, thus reducing the $h \to \gamma\gamma$ branching ratio. As shown in Figure 3, these regions shrink as M_h increases, since additional channels, in particular $gg \to h \to Z^0 Z^{0*} \to 4\ \ell$, become available for Higgs discovery.

These regions are reduced by considering either a larger data set or qqh Higgs production, in association with forward jets. An integrated luminosity of 100 fb^{-1} would remove the regions at large positive ξ in the $\Lambda_\phi = 5$ and 7.5 TeV plots of Fig. 2. Similarly, including the qqh, $h \to WW^* \to \ell\ell\nu\bar{\nu}$ channel in the list of the discovery modes removes the same two regions and reduces the large region of h non-observability at negative ξ values.

In all these regions, a complementarity is potentially offered by the process $gg \to \phi \to Z^0 Z^{0(*)} \to 4\ \ell$, which becomes important for $M_\phi > 140$ GeV. At the LHC, this process would have the same

event structure as the golden SM Higgs mode $H \to Z^0 Z^{0*} \to 4\ \ell$, which has been thoroughly studied for an intermediate mass Higgs boson. By computing the $gg \to \phi \to Z^0 Z^{0(*)} \to 4\ \ell$ rate relative to that for the corresponding SM H process and employing the LHC sensitivity curve for $H \to Z^0 Z^{0(*)}$ of Figure 1 (left), the significance for the ϕ signal in the 4 ℓ final state at the LHC can be extracted. Results are overlayed on Figures 2 and 3, assuming 30 fb^{-1} of data.

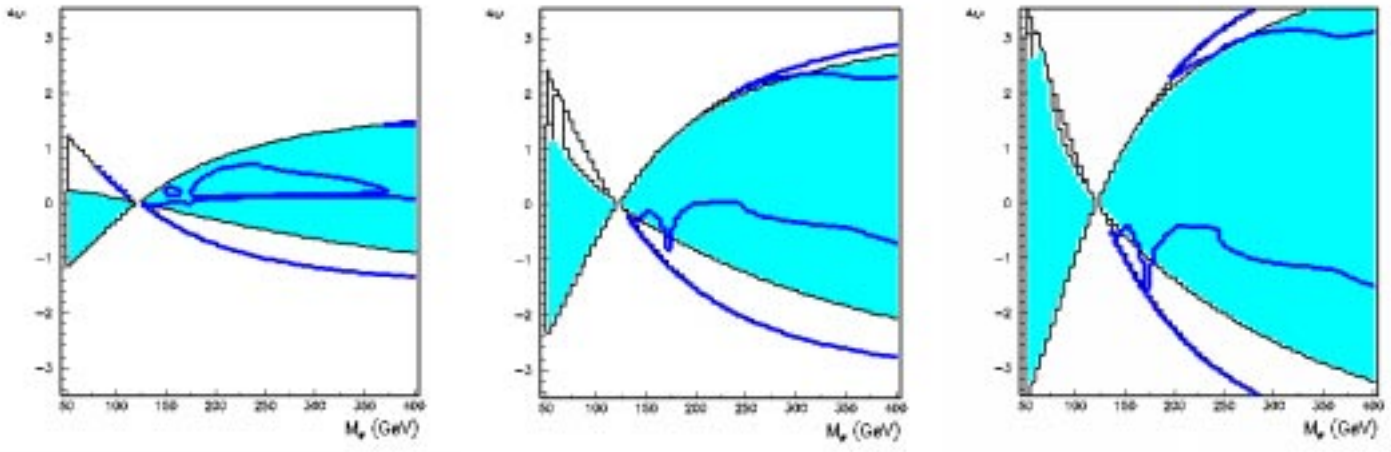

Figure 2: *Regions in (M_ϕ, ξ) parameter space of h detectability (including $gg \to h \to \gamma\gamma$ and other modes) and of $gg \to \phi \to Z^0 Z^{0(*)} \to 4\ \ell$ detectability at the LHC for one experiment and 30 fb^{-1}. The outermost, hourglass shaped contours define the theoretically allowed region. The light grey (cyan) regions show the part of the parameter space where the net h signal significance remains above 5 σ. In the empty regions between the shading and the outermost curves, the net h signal drops below the 5 σ level. The thick grey (blue) curves indicate the regions where the significance of the $gg \to \phi \to Z^0 Z^{0(*)} \to 4\ \ell$ signal exceeds 5 σ. Results are presented for M_h=120 GeV and Λ_ϕ= 2.5 TeV (left), 5.0 TeV (center) and 7.5 TeV (right).*

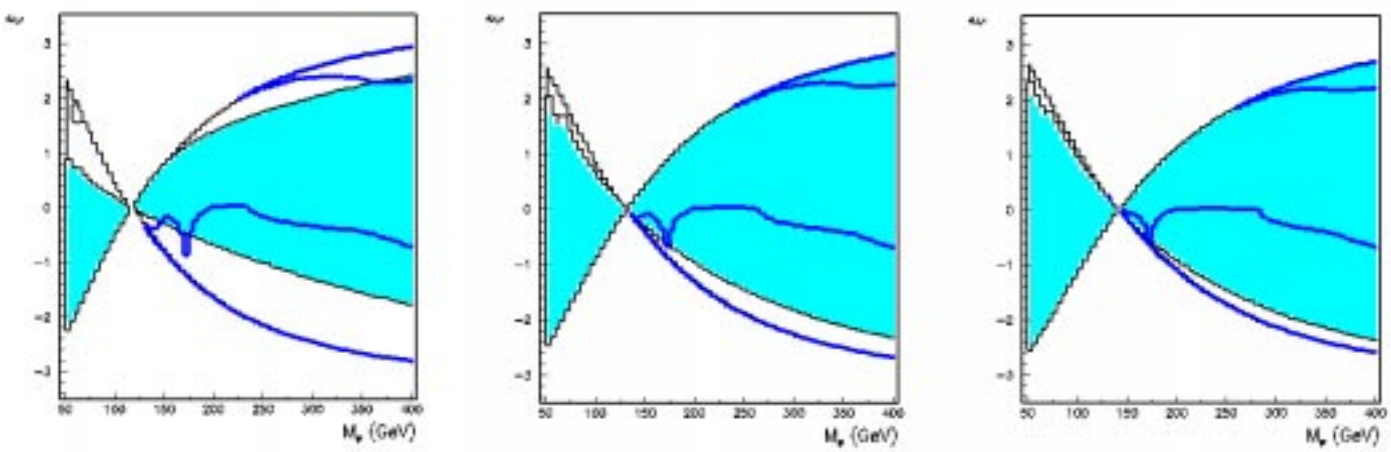

Figure 3: *Same as Figure 2 but for M_h = 115 GeV (left), M_h = 130 GeV (center) and M_h = 140 GeV (right). Λ_ϕ has been fixed to 5.0 TeV.*

Two observations are in order. The observability of ϕ production in the four lepton channel fills most of the gaps in (M_h, ξ) parameter space in which h detection is not possible (mostly due to the suppression of the loop-induced $gg \to h \to \gamma\gamma$ process). The observation of at least one scalar is thus guaranteed over almost the full parameter phase space, with the exception of: (a) the region of large positive ξ with $M_\phi < 140$ GeV, where the $\phi \to Z^0 Z^{0*}$ decay is phase-space-suppressed; and (b) a narrow region at $M_\phi \simeq 170$ GeV due to the ramp-up of the $\phi \to W^+W^-$ channel, where a luminosity of order 100 fb^{-1} is required to reach a $\geq 5\ \sigma$ signal for $\phi \to Z^0 Z^{0*}$. We should also note that the $\phi \to Z^0 Z^0$ decay is reduced for $M_\phi > 2M_h$ by the onset of the $\phi \to hh$ decay, which can become the main decay mode. The resulting $hh \to b\bar{b}b\bar{b}$ topology, with di-jet mass constraints, may represent a viable signal for the LHC in its own right, but detailed studies will be needed. Figures 2 and 3 also exhibit regions of (M_h, ξ) parameter space in which *both* the h and ϕ mass eigenstates will be detectable. In these regions, the LHC will observe two scalar bosons somewhat separated in mass with the lighter (heavier) having a non-SM-like rate for the the gg-induced $\gamma\gamma$ (Z^0Z^0) final state. Additional information will be required to ascertain whether these two Higgs bosons derive from a multi-doublet or other type of extended Higgs sector or from the present type of model with Higgs-radion mixing.

An e^+e^- LC should guarantee observation of both the h and the ϕ even in most of the regions within which detection of either at the LHC might be difficult. Thus, this scenario provides another illustration of the complementarity between the two machines in the study of the Higgs sector. In particular, in the region with $M_\phi > M_h$ the hZ^0Z^0 coupling is enhanced relative to the SM HZ^0Z^0 coupling and h detection in e^+e^- collisions would be even easier than SM H detection. Further, assuming that e^+e^- collisions could also probe down to $\phi Z^0 Z^0$ couplings of order $g^2_{\phi ZZ}/g^2_{HZZ} \simeq 0.01$, the ϕ would be seen in almost the entirety of the region for which ϕ detection at the LHC would not be possible. In this case, the measurements of the Z^0Z^0 boson couplings of both the Higgs and the radion particles would significantly constrain the values of the ξ and Λ_ϕ parameters of the model.

4.2 Determining the Nature of the Observed Scalar

The interplay between the emergence of the Higgs boson and of the radion graviscalar signals opens up the question of the identification of the nature of the newly observed particle(s).

After observing a new scalar at the LHC, some of its properties will be measured with sufficient accuracy to determine if they correspond to those expected for the SM H, i.e. for the minimal realization of the Higgs sector [18,19]. In the presence of extra dimensions, further scenarios emerge. For the present discussion, we consider two scenarios. The first has a light Higgs boson, for which we take $M_h = 120$ GeV, with couplings different from those predicted in the SM. The question here is if the anomaly is due to an extended Higgs sector, such as in Supersymmetry, or rather to the mixing with an undetected radion. The second scenario consists of an intermediate-mass scalar, with 180 GeV $< M <$ 300 GeV, observed alone. An important issue would then be the question of

whether the observed particle is the SM-like Higgs boson or a radion, with the Higgs particle left undetected. This scenario is quite likely at large negative ξ and large M_ϕ — see Figures 2 and 3.

In the first scenario, the issue is the interpretation of discrepancies in the measured Higgs couplings to gauge bosons and fermions. These effects increase with $|\xi|$, $1/\Lambda_\phi$ and M_h/M_ϕ. The LHC is expected to measure some ratios of these couplings [19]. In the case of the SM H, the ratio g_{HZZ}/g_{HWW} can be determined with a relative accuracy of 15% to 8% for 120 GeV $< M_H <$ 180 GeV, while the ratio $g_{H\tau\tau}/g_{HWW}$ and that of the effective coupling to photons, $g^{effective}_{H\gamma\gamma}/g_{HWW}$ can be determined to 6% to 10% for 120 GeV $< M_h <$ 150 GeV. Now, the Higgs-radion mixing would induce the same shifts in the direct couplings g_{hWW}, g_{hZZ} and $g_{h\bar{f}f}$, all being given by $d+\gamma b$ times the corresponding H couplings — see Eq. (7). Although this factor depends on the Λ_ϕ, M_ϕ and ξ parameters, ratios of couplings would remain unperturbed and correspond to those expected in the SM. Since the LHC measures mostly ratios of couplings, the presence of Higgs-radion mixing could easily be missed. One window of sensitivity to the mixing would be offered by the combination $g^{effective}_{h\gamma\gamma}/g_{hWW}$. But the mixing effects are expected to be limited to relative variation of $\pm 5\%$ w.r.t. the SM predictions. Hence, the LHC anticipated accuracy corresponds to deviations of one unit of σ, or less, except for a small region at $\Lambda_\phi \simeq 1$ TeV. Larger deviations are expected for the absolute rates [13], especially for the $gg \to h \to \gamma\gamma$ channel which can be dramatically enhanced or suppressed relative to the $gg \to H \to \gamma\gamma$ prediction for larger ξ values due to the large changes in the $gg \to h$ coupling relative to the $gg \to H$ coupling. Of course, to detect these deviations it is necessary to control systematic uncertainties for the absolute $\gamma\gamma$ rate. All the above remarks would also apply to distinguishing between the light Higgs of supersymmetry, which would be SM-like assuming an approximate decoupling limit, and the h of the Higgs-radion scenario. In a non-decoupling two-doublet model, the light Higgs couplings to up-type and down-type fermions can be modified differently with respect to those of the SM H, and LHC measurements of coupling ratios would detect this difference.

A TeV-class LC has the capability of extending the coupling measurements to all fermions separately with accuracies of order 1%-5% and achieves a determination of the total width to 4% - 6% accuracy [20]. This is important for the scenario we propose since it would provide enough measurements and sufficient accuracy to detect Higgs-radion mixing for moderate to large ξ values [21]. This is shown in Figure 4 by the additional contours, which indicate the regions where the discrepancy with the SM predictions for the Higgs couplings to pairs of b quarks and W bosons exceeds 2.5 σ. In particular, the *combination* of the direct observation of $\phi \to Z^0 Z^{0*}$ at the LHC and the precision measurements of the Higgs properties at a e^+e^- LC will extend our ability to distinguish between the Higgs-radion mixing scenario and the SM H scenario to a large portion of the regions where at the LHC only the h or only the ϕ is detected and determining that the observed boson is not the SM H is difficult. Further, close to the edges of the hourglass-shaped allowed region, the LC will also be able to detect ϕ production directly through the process $e^+e^- \to Z^0\phi$. In particular, this process will guarantee the observability of the ϕ in the low M_ϕ region, which is most difficult for the LHC.

If, at the LHC, an intermediate mass scalar is observed alone, its non-SM-like nature can, in some

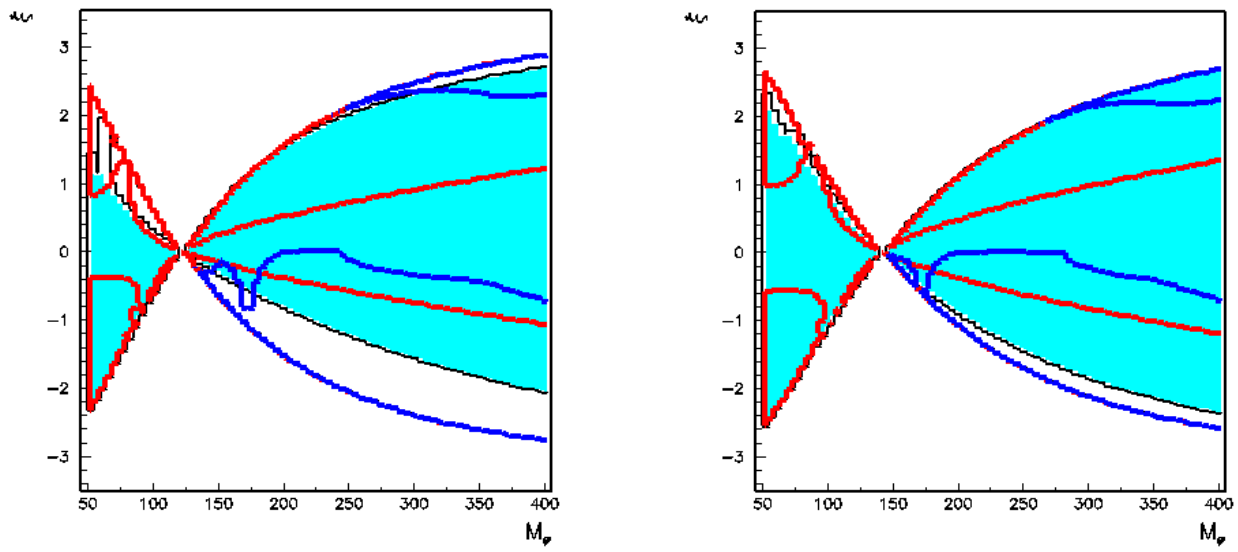

Figure 4: *Same as Figures 2 and 3 for M_h = 120 GeV (left), 140 GeV (right) and Λ_ϕ = 5 TeV with added contours, indicated by the medium grey (red) curves, showing the regions where the LC measurements of the h couplings to $b\bar{b}$ and W^+W^- would provide a $> 2.5\ \sigma$ evidence for the radion mixing effect. (Note: the grey (red) lines are always present along the outer edge of the hourglass in the $M_\phi > M_h$ region, but are sometimes buried under the darker (blue) curves. In this region, the $> 2.5\ \sigma$ regions lie between the outer hourglass edges and the inner grey (red) curves.)*

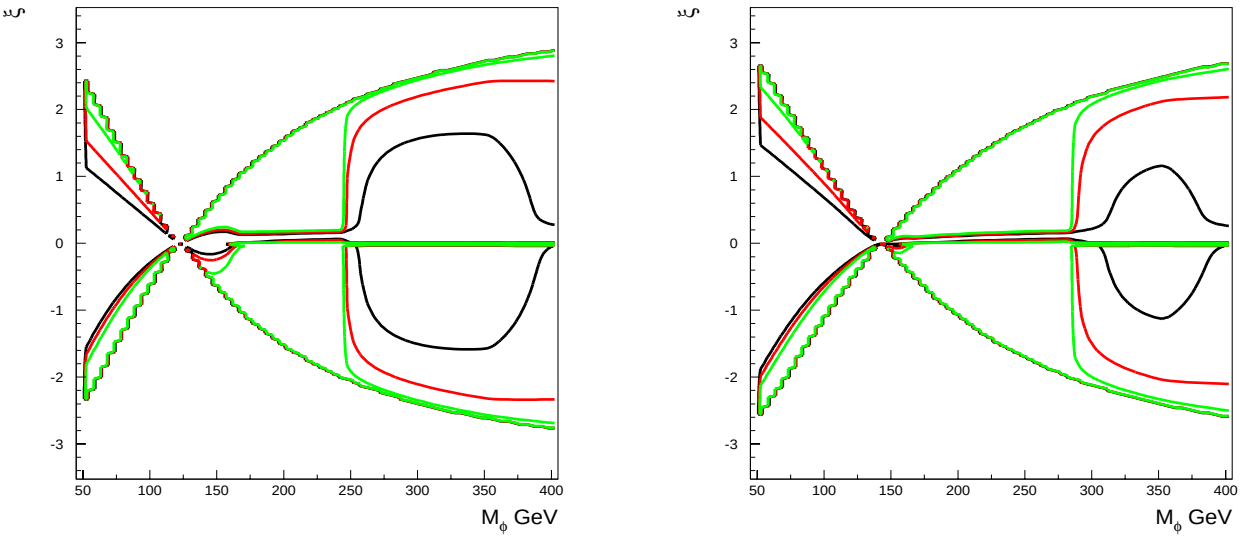

Figure 5: *Ratio $\frac{\mathrm{BR}(\phi \to Z^0 Z^{0(*)})}{\mathrm{BR}(H_{SM} \to Z^0 Z^{0(*)})}$ as function of M_ϕ and ξ. The curves indicate the 0.7 (black), 0.8 (medium grey/red) and 0.9 (light grey/green) contours. Results are obtained for M_h=120 GeV (left) and M_h = 140 GeV (right) and Λ_ϕ=5.0 TeV. The radion can be distinguished from the SM Higgs particle at intermediate values of its mass, past the threshold for the $\phi \to hh$ decay.*

cases, be determined through measurement of its production yield and its couplings. In particular, in the region at large, negative ξ values where ϕ production is visible whereas h production is not, the yield of $Z^0Z^0 \to 4\,\ell$ from ϕ decay can differ by a factor of 2 or more from that expected for a SM H (depending upon the value of M_ϕ — see Figure 13 of Ref. [13]). For M_ϕ such that $\phi \to hh$ decays are not allowed, the deviations arise from the substantial differences between the $gg \to \phi$ coupling and the $gg \to H$ coupling. For $M_\phi > 2M_h$ this rate is also sensitive to the exclusive branching fraction. Figure 5 shows the ratio of the $Z^0Z^{0(*)}$ decay branching fraction for the radion to that for the SM H. The figure shows that branching ratio differences are expected to be below 10% for radions with mass up to twice the Higgs mass. Such a small difference would not have a big impact compared to the possibly large deviations of $gg \to h/gg \to H$ relative to unity. However, past the threshold for $\phi \to hh$ decays, the Z^0Z^0 branching fraction is significantly affected away from $\xi \simeq 0$. The combination of a reduced $Z^0Z^0 \to 4\,\ell$ rate and the possibility to observe $\phi \to hh$ decays, ensures that the LHC could positively identify the existence of the radion in the region $M_\phi > 2M_h$, $\xi \neq 0$.

To conclude, we should note that the Higgs-radion sector is not the only means for probing the Randall-Sundrum type of model. The scenarios considered here will also yield the distinctive signature of KK graviton excitation production at the LHC [5]. This easily observed signal will serve as a warning to look for a possibly mixed Higgs-radion sector.

5 Conclusion

Perspectives for light Higgs searches at the LHC have been reviewed for models with warped extra dimensions, which introduce the radion graviscalar. The mixing of the Higgs field with the radion field induces changes in the production and decay properties of the Higgs boson mass eigenstate. Such changes may weaken, or even invalidate, the expectations obtained in earlier studies for observability of the Higgs boson. However, for almost the entire region of the parameter phase space where the suppression of the Higgs signal yield causes the overall signal significance at the LHC to drop below 5 σ, the radion eigenstate ϕ can be observed in the $gg \to \phi \to Z^0Z^{0(*)} \to 4\,\ell$ process instead. An e^+e^- linear collider would effectively complement the LHC both for the Higgs observability, including the most difficult region at low M_ϕ and positive ξ values, and for the detection of the radion mixing effects, through the precision measurements of the Higgs particle couplings to various types of particle pairs.

We wish to thank F. Gianotti, B. Grzadkowski, J. Hewett, A. Nikitenko, T. Rizzo and M. Toharia, for discussions and suggestions. JFG is supported by the U.S. Department of Energy and the Davis Institute for High Energy Physics.

References

[1] L. Randall, R. Sundrum, Phys. Rev. Lett. **83** (1999) 3370, [arXiv:hep-ph/9905221];
L. Randall, R. Sundrum, Phys. Rev. Lett. **83** (1999) 4690, [arXiv:hep-th/9906064].

[2] S. B. Bae, P. Ko, H. S. Lee and J. Lee, Phys. Lett. B **487** (2000) 299 [arXiv:hep-ph/0002224].

[3] H. Davoudiasl, J. L. Hewett and T. G. Rizzo, Phys. Rev. Lett. **84** (2000) 2080 [arXiv:hep-ph/9909255].

[4] K. Cheung, Phys. Rev. D **63** (2001) 056007 [arXiv:hep-ph/0009232].

[5] H. Davoudiasl, J. L. Hewett and T. G. Rizzo, Phys. Rev. D **63** (2001) 075004 [arXiv:hep-ph/0006041].

[6] S. C. Park, H. S. Song and J. Song, Phys. Rev. D **63** (2001) 077701 [arXiv:hep-ph/0009245].

[7] G. Giudice, R. Rattazzi, J. Wells, Nucl. Phys. B **595** (2001) 250 [arXiv:hep-ph/0002178].

[8] C. Csaki, M.L. Graesser, G.D. Kribs, Phys. Rev. D **63** (2001) 065002-1 [arXiv:hep-th/0008151].

[9] T. Han, G. D. Kribs and B. McElrath, Phys. Rev. D **64** (2001) 076003 [arXiv:hep-ph/0104074].

[10] M. Chaichian, A. Datta, K. Huitu and Z. h. Yu, Phys. Lett. B **524** (2002) 161 [arXiv:hep-ph/0110035].

[11] G. Azuelos, D. Cavalli, H. Przysiezniak and L. Vacavant, Eur. Phys. J. direct C **4** (2002) 16.

[12] J. L. Hewett and T. G. Rizzo, arXiv:hep-ph/0202155.

[13] D. Dominici, B. Grzadkowski, J. F. Gunion and M. Toharia, arXiv:hep-ph/0206192.

[14] J.J. van der Bij, Acta Physica Polonica, B **25** (1994) 827; R. Raczka, M. Pawlowski, Found. Phys. 24 (1994) 1305, [arXiv:hep-th/9407137].

[15] ATLAS Collaboration, *Detector and Physics Performance - Technical Design Report*, LHCC 99-14/15.

[16] A. Abdullin *et al.*, *Summary of the CMS Discovery Potential for the Higgs boson*, CMS Note in preparation.

[17] A. Djouadi, J. Kalinowski and M. Spira, Comput. Phys. Commun. **108** (1998) 56, [arXiv:hep-ph/9704448].

[18] D. Zeppenfeld, R. Kinnunen, A. Nikitenko and E. Richter-Was, Phys. Rev. D **62** (2000) 013009, [arXiv:hep-ph/0002036].

[19] D. Zeppenfeld, Int. J. Mod. Phys. A **16S1B** (2001) 831.

[20] M. Battaglia and K. Desch, Proc. of the 5^{th} *Int. Linear Collider Workshop LCWS 2000*, Fermilab, Batavia (IL), USA, AIP Conf. Proc. **578**, 163, [arXiv:hep-ph/0101165].

[21] T. G. Rizzo, arXiv:hep-ph/0209076.